Chen *et al*. *Complex Eng Syst* 2024;4:19
DOI: 10.20517/ces.2024.37

Complex Engineering Systems

Research Article

Open Access

Check for updates

Tobit Kalman fusion filtering under dynamic event-triggering protocol with token bucket specification

Xiangyu Chen[1,2], **Fei Han**[1,2,3,4], **Yanhua Song**[1,2], **Jinnan Zhang**[1,2,3]

[1]National Key Laboratory of Continental Shale Oil, Northeast Petroleum University, Daqing 163318, Heilongjiang, China.
[2]Artificial Intelligence Energy Research Institute, Northeast Petroleum University, Daqing 163318, Heilongjiang, China.
[3]Heilongjiang Provincial Key Laboratory of Networking and Intelligent Control, Northeast Petroleum University, Daqing 163318, Heilongjiang, China.
[4]Research Center for Mathematics and Interdisciplinary Sciences, Northeast Petroleum University, Daqing 163318, Heilongjiang, China.

Correspondence to: Dr. Yanhua Song, National Key Laboratory of Continental Shale Oil, Northeast Petroleum University, No. 99, Xuefu Street, High-Tech Industrial Development Zone, Daqing 163318, Heilongjiang, China. E-mail: hytsyh@126.com; ORCID: 0000-0002-3649-9160

How to cite this article: Chen X, Han F, Song Y, Zhang J. Tobit Kalman fusion filtering under dynamic event-triggering protocol with token bucket specification. *Complex Eng Syst* 2024;4:19. http://dx.doi.org/10.20517/ces.2024.37

Received: 23 Jun 2024 **First Decision:** 14 Aug 2024 **Revised:** 5 Sep 2024 **Accepted:** 8 Oct 2024 **Published:** 22 Oct 2024

Academic Editor: Hamid Reza Karimi **Copy Editor:** Fangling Lan **Production Editor:** Fangling Lan

Abstract

This paper addresses the multi-sensor fusion filtering problem for a class of linear discrete time-varying systems with censored measurement, described by the Tobit model, and scheduled by dynamic event-triggering protocols with token bucket specification. A dynamic event-triggering mechanism is first used to determine whether to transmit measurements under the token bucket specification, allowing transmission only if there are sufficient tokens and if the event-triggering condition is satisfied. Next, two indicator variables are denoted to represent the combined impact of the dynamic event-triggering protocol and the token bucket specification. A local Tobit Kalman filtering algorithm is then designed for each node by minimizing the trace of the filtering error covariance matrix under censoring and information transmission protocols' influence. Subsequently, all local estimates from each node are transmitted to the fusion center, where global estimates are generated using a federal fusion rule. The global estimates with suitable weights are sent back to every node for predictions at subsequent time instants. Finally, an illustrative simulation example is used to evaluate performance of this fused filtering scheme proposed in this paper.

Keywords: Tobit Kalman filtering, token bucket protocol, censored measurements, multi-sensor filtering fusion

1. INTRODUCTION

As is well known, multi-sensor fusion filtering (MSFF) refers to the integration of information from different sensors to enhance the performance of the filtering scheme [1]. To date, multi-sensor information fusion technology has been extensively applied in a variety of fields, including target localization [2,3], fault detection [4], environmental monitoring [5], signal processing [6], image processing [7], *etc*. In general, multi-sensor fusion falls into two categories: centralized and distributed [8]. In the former, the raw data from each sensor is directly transmitted to the fusion center for filtering processing [9]. In contrast, the latter manner involves the fusion center integrating available estimates from local filters to generate optimal or suboptimal estimates [10]. While the precision of distributed fusion filtering may not match that of centralized fusion, its advantages include reducing the burden on the central processor, lowering communication bandwidth requirements, and enhancing system reliability and robustness. These distinguished advantages have led to widespread attention towards distributed fusion filtering schemes in recent years [11].

In networked control systems, due to harsh environmental conditions, limitations in sensor capabilities, poor signal transmission line quality, and hardware or software failures in sensors, nonlinearities are inevitable in the actual system measurement output. These nonlinearities include, but are not limited to, censoring [12], channel fading [13], quantization [14], saturation [15], *etc*. If not handled properly, these nonlinear factors may even affect the stability of the filtering error system. When designing and implementing filters in networked systems, it is necessary to fully consider the impact of these nonlinear factors and take effective measures to minimize their impact on system performance to ensure system stability and reliability. At present, for addressing nonlinear challenges and improving filtering accuracy and stability, various nonlinear filtering algorithms have been proposed, such as the extended Kalman filtering (EKF) [16], the unscented Kalman filtering (UKF) [17], and the Tobit Kalman filtering (TKF) [18].

Because of the limited sensing abilities of low-cost sensors, the censored measurements are prevalent in practical engineering [19]. The censored measurements are commonly formulated by the Tobit model, which is widely used in data analysis in economics, finance, and social sciences. This model can effectively handle problems involving censored data and provides estimates of unobserved variables. When the measurement noise of a system exhibits non-Gaussian characteristics near the censoring region, traditional Kalman filtering methods cannot handle it. The primary challenge induced by the censored measurements lies in its nonlinearities. A useful method is to introduce the indicator variable to transform the piecewise linear functions into a unified form in [20], which will provide convenience for performance analysis and deal with the scalable distributed $H\infty$-consensus filtering problem. Another challenge in recursive filtering is to calculate the probability of occurrence of censoring measurement [21]. In addition, the TKF surpasses both UKF and EKF in terms of filtering performance when dealing with censored measurements [22].

Allik *et al*. have designed TKF for the first time by using the Tobit model, where the unilateral and bilateral Tobit regression models are integrated into the recursive form of the Kalman filter [23]. In a comparison of TKF and KF, it can be found that when data is not censored, there is no difference between these two filters; when data is censored, the extra computational burden of TKF mainly comes from the calculation of occurrence of censoring measurement. Nevertheless, it fails to fully explore and utilize the useful information contained in the censored region. To address this problem, Han *et al*. have developed a novel conditional expectation approach to study TKF problem for stochastic parameter systems [24]. Subsequent research regarding TKF has been published by combining with other interesting phenomena, such as dynamic bias and Round-Robin protocol [25], fading measurements [26], dynamic event-triggered protocols (DETPs) [27], and so on.

Although there are currently a large number of research results on TKF, the Tobit Kalman fusion filtering (TKFF) has not received sufficient attention due primarily to its complexities in analysis. The core step of this paper is to select an appropriate fusion rule from various existing fusion rules and combine it with local TKFs.

The well-known fusion rules include centralized filtering fusion [28], information filtering fusion [29], weighted filtering fusion [30], covariance intersection fusion [31], federated filtering fusion [10], sequential fusion [32], and robust fusion [33]. In the survey paper [34], these fusion rules are compared in terms of the structure of the fusion, filtering accuracy, and computation burden, respectively. Federated filtering fusion belongs to a distributed structure and has the smallest burden and highest burden. As a result, we choose federated filtering fusion for this paper.

In the past decades, networked systems have gained popularity owing to multiple advantages such as high flexibility, simple installation, and low cost, making them suitable for a range of applications including aerospace, energy monitoring, and telecommunications [35]. Unlike traditional automatic control systems, the focus of networked systems explicitly considers the limitations of the communication medium between the sensor and the controller/filter. Especially when network congestion occurs, where the allocation of requests exceeds the network's sustainable transmission rate, these limitations become even more evident, which would pose a serious impact on the desirable performance. A well-established paradigm for addressing this issue is event-triggered protocol [36]. The idea of event-triggered protocol is to reduce the transmission number only if the event-triggering condition is satisfied. Such a protocol can efficiently save the communication resource [37]. However, it cannot be guaranteed that the transmission network will not be overused, especially when the desired performance level requires a high transmission rate. In the existing references [36,37], the event-triggering protocol (ETP) is introduced to save unilaterally the network bandwidth resource in the premise of a certain performance by reducing the number of information transmissions. Nonetheless, such a protocol cannot be appropriate for practical engineering scenarios. In a shared network with limited bandwidth, when encountering multiple requests of information transmission, it is difficult to have enough bandwidth resources.

It should be noted that the total communication resource cannot be formulated in the existing results and thus the role of the ETP cannot be reflected in a unified framework. Recently, a dynamic model has been used to describe the network resources: the token bucket algorithm [38,39], where the network's communication resources are considered and the signal transmission is triggered only when the network's communication capabilities allow. The level of the bucket reflects the network's current communication capabilities. The objective of these studies is to optimally utilize limited communication resources by combining control inputs with triggering mechanisms [40]. Inspired by such an idea, an interesting problem is to explore how the token bucket algorithm can be integrated with communication protocols, to more reasonably allocate tokens for network requests and achieve optimized resource utilization. In line with this concept, an intriguing issue is to investigate the integration of the token bucket algorithm with DETPs within a unified framework for studying TKFF. This constitutes another motivation for the present paper.

Enlightened by the above arguments, the objective is to investigate the federated TKFF (FTKFF) problem under the schedule of dynamic event-triggered protocols with token bucket specification. The main contributions of this paper are highlighted as follows: (1) an FTKFF problem is studied under the combined schedule of the token buckets and DETPs, where the former characterizes the limited communication resources and the latter determines the necessary information to be transmitted; (2) a recursive local filter is designed, where two indicator variables are introduced to formulate the transmitted censored measurements, and the gain matrix is derived by minimizing the upper bound of the filtering error covariance; (3) the federated fusion criterion is chosen in the fusion center to obtain an optimal estimation by using the local estimates.

Notations: $\|x\| = \sqrt{x^T x}$, where $x \in \mathbb{R}^n$. The notation $X > Y$, where X and Y are real symmetric matrices, means that $X - Y$ is positive-definite. $\mathrm{tr}\{X\}$ stands for the trace of the matrix X. $\mathbb{E}\{\cdot\}$ and $\mathbb{D}\{\cdot\}$ are the mathematical expectation and variance. $\delta(\cdot) \in (0, 1)$ is the Dirac delta function.

2. PROBLEM FORMULATION

2.1. System model

Consider the state-space model for a class of linear discrete time-varying systems and its measurements from l sensor nodes as follows:

$$\begin{cases} x_{t+1} = A_t x_t + B_t \omega_t, \\ z_{m,t} = C_{m,t} x_t + v_{m,t}, m = 1, 2, \ldots, l \end{cases} \tag{1}$$

where $x_t \in \mathbb{R}^{n_x}$ and $z_{m,t} \in \mathbb{R}^{n_y}$ are the state vector and measurement vector, respectively; $\omega_t \in \mathbb{R}^{\omega}$ and $v_{m,t} \in \mathbb{R}^{n_y}$ are white Gaussian noises with $\mathbb{E}\{\omega_t\} = 0$, $\mathbb{E}\{v_{m,t}\} = 0$, $\mathbb{D}\{\omega_t\} = Q_t$, and $\mathbb{D}\{v_{m,t}\} = R_{m,t}$. Furthermore, it is assumed that x_0, ω_t and $v_{m,t}$ are mutually independent for different t and m. A_t, B_t and $C_{m,t}$ are known time-varying matrices with compatible dimensions; the initial state x_0 is a random variable with mean $\bar{x}_0$ and variance P_0. For convenience of later discussion, denote $z_{m,t} \triangleq \begin{bmatrix} z_{m,t}^{(1)} & z_{m,t}^{(2)} & \ldots & z_{m,t}^{(n_y)} \end{bmatrix}^T \in \mathbb{R}^{n_y}$.

The situation where one or multiple sensors cannot perform data measurement or acquisition properly for various reasons is referred to as "censored measurements". To address the issue of censored measurements and mitigate its adverse impact on system monitoring, the Tobit measurement model is used to formulate the one-side censored measurement:

$$y_{m,t}^{(j)} \triangleq \begin{cases} z_{m,t}^{(j)}, & z_{m,t}^{(j)} > \tau_m^{(j)}; \\ \tau_m^{(j)}, & z_{m,t}^{(j)} \le \tau_m^{(j)} \end{cases} \tag{2}$$

where $y_{m,t}^{(j)}$ is the censored measurement from the m-th sensor and $\tau_m^{(j)}$ is the one-side censoring threshold of $y_{m,t}^{(j)}$.

In light of (2), define a series of Bernoulli random variables $\varrho_{m,t}^{(j)} (m = 1, 2, \ldots, l; j = 1, 2, \ldots, n_y)$ to formulate $y_{m,t}^{(j)}$ as follows:

$$\varrho_{m,t}^{(j)} \triangleq \begin{cases} 1, & z_{m,t}^{(j)} > \tau_m^{(j)}; \\ 0, & z_{m,t}^{(j)} \le \tau_m^{(j)}, \end{cases} \tag{3}$$

which obeys the distribution law:

$$\begin{cases} \mathbb{P}\{\varrho_{m,t}^{(j)} = 1\} = \bar{\varrho}_{m,t}^{(j)}; \\ \mathbb{P}\{\varrho_{m,t}^{(j)} = 0\} = 1 - \bar{\varrho}_{m,t}^{(j)} \end{cases} \tag{4}$$

where $\bar{\varrho}_{m,t}^{(j)}$ are known non-negative constants. Moreover, $\varrho_{m,t}$ is uncorrelated with other random variables mentioned above.

The censoring probability $\bar{\varrho}_{m,t}$ is approximated by

$$\bar{\varrho}_{m,t}^{(j)} = \Phi\left(\frac{(C_{m,t} x_t)^{(j)} - \tau_m^{(j)}}{\sqrt{R_{m,t}^{(j)}}} \right) \approx \Phi\left(\frac{(C_{m,t} \hat{x}_{m,t|t-1})^{(j)} - \tau_m^{(j)}}{\sqrt{R_{m,t}^{(j)}}} \right) \tag{5}$$

where $\hat{x}_{m,t|t-1}$ represents prediction for x_t from node m, and $\Phi(\cdot)$ is the cumulative distribution function of the standard normal distribution. From (5), it follows that $\bar{\varrho}_{m,t}$ is related to the state x_t, which is replaced with $\hat{x}_{m,t|t-1}$ since x_t is unknown.

Similar to [12], the measurement expectation and variance of $\bar{\varrho}_{m,t}^{(j)}$ are given as follows:

$$\mathbb{E}\{y_{m,t}^{(j)} | x_t\} = \Phi\left(\frac{(C_{m,t} x_t)^{(j)} - \tau_m^{(j)}}{\sqrt{R_{m,t}^{(j)}}} \right) \left[(C_{m,t} x_t)^{(j)} + \sqrt{R_{m,t}^{(j)}} \lambda \left(\frac{\tau_m^{(j)} - (C_{m,t} x_t)^{(j)}}{\sqrt{R_{m,t}^{(j)}}} \right) \right] + \Phi\left(\frac{\tau_m^{(j)} - (C_{m,t} x_t)^{(j)}}{\sqrt{R_{m,t}^{(j)}}} \right) \tau_m^{(j)}, \tag{6}$$

$$\mathbb{D}\{y_{m,t}^{(j)}|x_t\} = R_{m,t}^{(j)}\left[1-\varphi\left(\frac{\tau_m^{(j)}-(C_{m,t}x_t)^{(j)}}{\sqrt{R_{m,t}^{(j)}}}\right)\right] \tag{7}$$

where

$$\lambda(\zeta) \triangleq \frac{\phi(\zeta)}{1-\Phi(\zeta)}, \quad \varphi(\zeta) \triangleq \lambda(\zeta)(\lambda(\zeta)-\zeta).$$

Here, $\phi(\cdot)$ and $\Phi(\cdot)$ are the probability density function and the cumulative distribution function of the standard normal distribution, respectively.

Denote $\varrho_{m,t} \triangleq \mathrm{diag}\left\{\varrho_{m,t}^{(1)}, \varrho_{m,t}^{(2)}, \ldots, \varrho_{m,t}^{(n_y)}\right\}$, $y_{m,t} \triangleq \left[y_m^{(1)}, y_m^{(2)}, \ldots, y_m^{(n_y)}\right]^T$, and $\tau_m \triangleq \left[\tau_m^{(1)}, \tau_m^{(2)}, \ldots, \tau_m^{(n_y)}\right]^T$. Hence, (2) can be rewritten as:

$$y_{m,t} = \varrho_{m,t} z_{m,t} + (I-\varrho_{m,t})\tau_m. \tag{8}$$

Also, the following statistical information can be obtained from (6) and (7):

$$\mathbb{E}\{y_{m,t}|x_t\} = \Phi\left(\frac{C_{m,t}x_t-\tau_m}{\sqrt{R_{m,t}}}\right)\left[C_{m,t}x_t+\sqrt{R_{m,t}}\lambda\left(\frac{\tau_m-C_{m,t}x_t}{\sqrt{R_{m,t}}}\right)\right]+\Phi\left(\frac{\tau_m-C_{m,t}x_t}{\sqrt{R_{m,t}}}\right)\tau_m, \tag{9}$$

and

$$\mathbb{D}\{y_{m,t}|x_t\} = R_{m,t}\left[I-\varphi\left(\frac{\tau_m-C_{m,t}x_t}{\sqrt{R_{m,t}}}\right)\right]. \tag{10}$$

Remark 1. *The censoring measurement is formulated as the Tobit model. The main challenge in dealing with the Tobit model arises from two aspects. Firstly, the Tobit model* (2) *represents a piecewise linear function, which is inherently nonlinear. To facilitate subsequent analysis, a random variable defined in* (3) *is introduced to reformulate the censoring measurement into a uniform form* (8)*. Another issue involves determining the probability law and statistical property of the random variable (i.e.,* (5)*,* (6)*, and* (7)*), where* (5) *is derived by using statistical information of normal distribution of measurement noise* $v_{m,t}$*, and* (6) *and* (7) *are achieved by means of* (5)*.*

2.2. Information transmission protocols

To save precious energy and limited bandwidth, the DETP is used for node m to decide whether to transmit the current measurements to the filter. For this purpose, denote the event-triggering time sequence by $0 \le t_m^1 < \cdots < t_m^n < \cdots$ and define

$$t_m^{n+1} \triangleq \min\left\{t|t > t_m^n, \frac{1}{\chi_m}\eta_{m,t}+\sigma_m-\|\varepsilon_{m,t}\| \le 0\right\}, \tag{11}$$

$$\varepsilon_{m,t} \triangleq y_{m,t_m^n} - y_{m,t}, \tag{12}$$

where σ_m and χ_m are given positive scalars, y_{m,t_m^n} represents the latest transmitted measurement until time t, and the internal dynamic variable $\eta_{m,t}$ satisfies:

$$\eta_{m,t+1} = \lambda_m\eta_{m,t}+\sigma_m-\|\varepsilon_{m,t}\|, \quad \eta_{m,0}=\eta_0, \tag{13}$$

where λ_m is a given positive scalar and $\eta_0 \ge 0$ is the initial value. Moreover, $\lambda_m\chi_m > 1$ and thus ensure $\eta_{m,t+1} \ge 0$. Here, the inequality

$$\frac{1}{\chi_m}\eta_{m,t}+\sigma_m-\|\varepsilon_{m,t}\| \le 0, \tag{14}$$

is referred to as the event-triggering condition. For convenience, define the following indicator variable:

$$\alpha_{m,t} \triangleq \begin{cases} 1, & \text{if (14) holds ;} \\ 0, & \text{otherwise.} \end{cases} \tag{15}$$

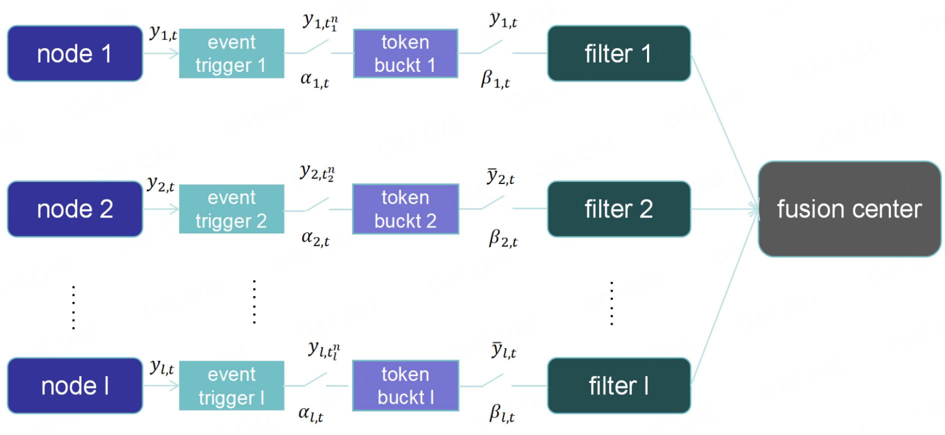

Figure 1. A block diagram of FTKFF under DETP with token bucket.

To cope with the measurement transmission in unexpected situations, such as the need to transfer multiple data at once, a token bucket triggering mechanism is introduced. First, the token bucket is employed to describe the available bandwidth resource, where the integer g and c_m are the token generating rate and transmission cost, respectively. For simplicity, c_m means the total cost for transmitting all elements of $y_{m,t}$ at time instant t of node m.

In order to unify the centralized utilization of the token bucket algorithm, the number of tokens is then evenly allocated to each sensor node, which is given as follows:

$$\xi_{m,t} = \xi_t / l. \tag{16}$$

The internal token change of the token bucket is formulated as follows:

$$\xi_t = \min\left\{\xi_{t-1} + g - \sum_{m=1}^{l} \beta_{m,t}\alpha_{m,t}c_m, b\right\} \tag{17}$$

with initial values $\xi_0 \geq 0$, where b is the token bucket capacity, and

$$\beta_{m,t} \triangleq \begin{cases} 1, & \text{if } c_m \leq \xi_{m,t}; \\ 0, & \text{otherwise.} \end{cases} \tag{18}$$

After scheduled by the DETP with token bucket specification, the measurement received by the filter is formulated as

$$\bar{y}_{m,t} = \begin{cases} y_{m,t_m^n}, & \text{if } \beta_{m,t} = 1 \text{ and } \alpha_{m,t} = 1; \\ \bar{y}_{m,t-1}, & \text{otherwise.} \end{cases} \tag{19}$$

For the convenience of later analysis, (19) is rewritten as

$$\bar{y}_{m,t} = \alpha_{m,t}\beta_{m,t}y_{m,t_m^n} + (1 - \alpha_{m,t}\beta_{m,t})\bar{y}_{m,t-1}. \tag{20}$$

Remark 2. *Different from*[30]*, the introduction of the indicator variable* $\alpha_{m,t}$ *is utilized to determine whether the conditions are met. This approach provides convenience for subsequent analysis, clearly defining the impact of the ETP. Building on this concept, another indicator variable* $\beta_{m,t}$ *is implemented to assess whether there are sufficient tokens for information transmission.*

The block diagram of FTKFF is depicted in Figure 1. As for node m, the event trigger is used to determine whether the censored measurement $y_{m,t}$ is transmitted or not, which is formulated by $\alpha_{m,t}$. If the event-triggering condition (14) to be predetermined is met (i.e., $\alpha_{m,t} = 1$), then the measurement to be transmitted is denoted as y_{m,t_m^n}. Next, the token bucket m is employed to formulate the available communication resource, which is formulated by $\beta_{m,t}$. If there exist sufficient tokens (i.e., $\beta_{m,t} = 1$), then the filter can receive the measurement, i.e., $\bar{y}_{m,t}$. Therefore, only when both token and event-triggering conditions are met can information transmission proceed. Such a procedure is expressed as (20).

2.3. Filter design

By using the available measurement $\bar{y}_{m,t}$, construct a recursive filter

$$\hat{x}_{m,t|t-1} = A_{t-1}\hat{x}_{m,t-1|t-1}, \tag{21}$$

$$\hat{x}_{m,t|t} = \hat{x}_{m,t|t-1} + K_{m,t}(\bar{y}_{m,t} - \hat{y}_{m,t|t-1}) \tag{22}$$

with the initial value $\hat{x}_{m,0|0} = \bar{x}_{m,0}$, and for $t \in [t_m^n, t_m^{n+1})(n \geq 0, t \geq 1)$, where $\hat{x}_{m,t|t-1}$ and $\hat{x}_{m,t|t}$ represent the prediction of one step and estimation from node m, respectively; $\hat{y}_{m,t|t-1}$ is the measurement estimate to be discussed later; and $K_{m,t}$ is the filter gain to be designed.

The primary objective of this paper is to design a local filter of the form (21) and (22) for every node under the DETP with token bucket specifications for all censored measurements within the framework of TKF. Moreover, we are devoted to developing an FTKFF framework to address the multiple challenges induced by the censored measurements, the DETP and the token bucket specifications.

3. MAIN RESULTS

This section introduces the recursive bound of the TKF of the filtering error covariance. In addition, the desired filter gain is calculated based on the minimum mean square error criterion.

3.1. Filtering error and covariance matrix

In line with (5) and (6), the estimate of the measurement $\hat{y}_{m,t|t-1}$ is derived as

$$\hat{y}_{m,t|t-1} = \bar{\varrho}_{m,t}(C_{m,t}\hat{x}_{m,t|t-1} + \lambda_{m,t}\sqrt{\mathcal{R}_{m,t}}) + (I - \bar{\varrho}_{m,t})\tau_m \tag{23}$$

where

$$\bar{\varrho}_{m,t} \triangleq \mathrm{diag}\left\{\bar{\varrho}_{m,t}^{(1)}, \bar{\varrho}_{m,t}^{(2)}, \dots, \bar{\varrho}_{m,t}^{(n_y)}\right\}, \qquad \lambda_{m,t} \triangleq \lambda\left(\frac{\tau_m - C_{m,t}\hat{x}_{m,t|t-1}}{\sqrt{R_{m,t}}}\right),$$
$$\mathcal{R}_{m,t} \triangleq \begin{bmatrix} R_{m,t}^{(1)} & \cdots & R_{m,t}^{(n_y)} \end{bmatrix}^T, \qquad \sqrt{\mathcal{R}_{m,t}} \triangleq \begin{bmatrix} \sqrt{R_{m,t}^{(1)}} & \cdots & \sqrt{R_{m,t}^{(n_y)}} \end{bmatrix}^T.$$

Let $e_{m,t|t-1} \triangleq x_t - \hat{x}_{m,t|t-1}$. From (1) and (21), one calculates

$$e_{m,t|t-1} = A_{t-1}e_{m,t-1|t-1} + B_{t-1}\omega_{t-1}. \tag{24}$$

Subsequently, from (1), (8), (22) and (23), one has

$$\begin{aligned} e_{m,t|t} =& (I - K_{m,t}\bar{\varrho}_{m,t}C_{m,t})e_{m,t|t-1} - (1-\theta_{m,t})K_{m,t}\varrho_{m,t}v_{m,t} + K_{m,t}\bar{\varrho}_{m,t}\lambda_{m,t}\sqrt{\mathcal{R}_{m,t}} \\ & - (1-\theta_{m,t})K_{m,t}\tilde{\varrho}_{m,t}C_{m,t}x_t + \theta_{m,t}K_{m,t}\bar{\varrho}_{m,t}C_{m,t}x_t - \theta_{m,t}K_{m,t}\bar{y}_{m,t-1} \\ & - (1-\theta_{m,t})K_{m,t}\varepsilon_{m,t} + \theta_{m,t}K_{m,t}(I - \bar{\varrho}_{m,t})\tau_m + (1-\theta_{m,t})K_{m,t}\tilde{\varrho}_{m,t}\tau_m \end{aligned} \tag{25}$$

where

$$\theta_{m,t} \triangleq 1-\alpha_{m,t}\beta_{m,t},\ \tilde{\varrho}_{m,t} \triangleq \varrho_{m,t}-\bar{\varrho}_{m,t},\ \varepsilon_{m,t} \triangleq y_{m,t_m^n}-y_{m,t}.$$

By means of Eqs. (24) and (25), the covariance matrices of the prediction error and filtering error are, respectively, calculated as follows

$$P_{m,t|t-1}=\mathbb{E}(e_{m,t|t-1}e_{m,t|t-1}^T)=A_{t-1}P_{m,t-1|t-1}A_{t-1}^T+B_{t-1}Q_{t-1}B_{t-1}^T, \tag{26}$$

and

$$\begin{aligned}P_{m,t|t}=&(I-K_{m,t}\bar{\varrho}_{m,t}C_{m,t})P_{m,t|t-1}(I-K_{m,t}\bar{\varrho}_{m,t}C_{m,t})^T+(1-\theta_{m,t})^2K_{m,t}\mathbb{E}\{\varrho_{m,t}v_{m,t}v_{m,t}^T\varrho_{m,t}^T\}K_{m,t}^T\\&+K_{m,t}\bar{\varrho}_{m,t}\mathbb{E}\Big\{\lambda_{m,t}\sqrt{\mathcal{R}_{m,t}}\sqrt{\mathcal{R}_{m,t}}^T\lambda_{m,t}^T\Big\}\bar{\varrho}_{m,t}^TK_{m,t}^T+(1-\theta_{m,t})^2K_{m,t}\mathbb{E}\{\tilde{\varrho}_{m,t}C_{m,t}x_tx_t^TC_{m,t}^T\tilde{\varrho}_{m,t}^T\}K_{m,t}^T\\&+\theta_{m,t}^2K_{m,t}\bar{\varrho}_{m,t}\mathbb{E}\{C_{m,t}x_tx_t^TC_{m,t}^T\}\bar{\varrho}_{m,t}^TK_{m,t}^T+\theta_{m,t}^2K_{m,t}\mathbb{E}\{\bar{y}_{m,t-1}\bar{y}_{m,t-1}^T\}K_{m,t}^T+\mathcal{K}_{m,t}^1+\mathcal{K}_{m,t}^{1^T}\\&+(1-\theta_{m,t})^2K_{m,t}\mathbb{E}\{\varepsilon_{m,t}\varepsilon_{m,t}^T\}K_{m,t}^T+\theta_{m,t}^2K_{m,t}(I-\bar{\varrho}_{m,t})\mathbb{E}\{\tau_m\tau_m^T\}(I-\bar{\varrho}_{m,t})^TK_{m,t+1}^T\\&+(1-\theta_{m,t})^2K_{m,t}\mathbb{E}\{\tilde{\varrho}_{m,t}\tau_m\tau_m^T\tilde{\varrho}_{m,t}^T\}K_{m,t}^T+\mathcal{K}_{m,t}^2+\mathcal{K}_{m,t}^{2^T}-\mathcal{K}_{m,t}^3-\mathcal{K}_{m,t}^{3^T}-\mathcal{K}_{m,t}^4-\mathcal{K}_{m,t}^{4^T}\\&+\mathcal{K}_{m,t}^5+\mathcal{K}_{m,t}^{5^T}+\mathcal{K}_{m,t}^6+\mathcal{K}_{m,t}^{6^T}+\mathcal{K}_{m,t}^7+\mathcal{K}_{m,t}^{7^T}-\mathcal{K}_{m,t}^8-\mathcal{K}_{m,t}^{8^T}+\mathcal{K}_{m,t}^9+\mathcal{K}_{m,t}^{9^T}-\mathcal{K}_{m,t}^{10}-\mathcal{K}_{m,t}^{10^T}\\&-\mathcal{K}_{m,t}^{11}-\mathcal{K}_{m,t}^{11^T}-\mathcal{K}_{m,t}^{12}-\mathcal{K}_{m,t}^{12^T}+\mathcal{K}_{m,t}^{13}+\mathcal{K}_{m,t}^{13^T}\end{aligned} \tag{27}$$

where

$$\begin{aligned}\mathcal{K}_{m,t}^1&\triangleq\mathbb{E}\{(I-K_{m,t}\bar{\varrho}_{m,t}C_{m,t})e_{m,t|t-1}\sqrt{\mathcal{R}_{m,t}}^T\lambda_{m,t}^T\bar{\varrho}_{m,t}^TK_{m,t}^T\},\\\mathcal{K}_{m,t}^2&\triangleq\theta_{m,t}\mathbb{E}\{(I-K_{m,t}\bar{\varrho}_{m,t}C_{m,t})e_{m,t|t-1}x_t^TC_{m,t}^TK_{m,t}^T\bar{\varrho}_{m,t}^T\},\\\mathcal{K}_{m,t}^3&\triangleq\theta_{m,t}\mathbb{E}\{(I-K_{m,t}\bar{\varrho}_{m,t}C_{m,t})e_{m,t|t-1}\bar{y}_{m,t-1}^TK_{m,t}^T\},\\\mathcal{K}_{m,t}^4&\triangleq(1-\theta_{m,t})\mathbb{E}\{(I-K_{m,t}\bar{\varrho}_{m,t}C_{m,t})e_{m,t|t-1}\varepsilon_{m,t}^TK_{m,t}^T\},\\\mathcal{K}_{m,t}^5&\triangleq\theta_{m,t}\mathbb{E}\{(I-K_{m,t}\bar{\varrho}_{m,t}C_{m,t})e_{m,t|t-1}\tau_{m,t}^T(I-\bar{\varrho}_{m,t})^TK_{m,t}^T\},\\\mathcal{K}_{m,t}^6&\triangleq(1-\theta_{m,t})^2\mathbb{E}\{K_{m,t}\tilde{\varrho}_{m,t}C_{m,t}x_t\tau_m^T\tilde{\varrho}_{m,t}^TK_{m,k}^T\},\\\mathcal{K}_{m,t}^7&\triangleq\theta_{m,t}\mathbb{E}\{K_{m,t}\bar{\varrho}_{m,t}C_{m,t}x_t\sqrt{\mathcal{R}_{m,t}}^T\lambda_{m,t}^T\bar{\varrho}_{m,t}^TK_{m,t}^T\},\\\mathcal{K}_{m,t}^8&\triangleq\theta_{m,t}^2\mathbb{E}\{K_{m,t}\bar{\varrho}_{m,t}C_{m,t}x_t\bar{y}_{m,t-1}^TK_{m,t-1}^T\},\\\mathcal{K}_{m,t}^9&\triangleq\theta_{m,t}^2\mathbb{E}\{K_{m,t}\bar{\varrho}_{m,t}C_{m,t}x_t\tau_m^T(I-\bar{\varrho}_{m,t})^TK_{m,t}^T\},\\\mathcal{K}_{m,t}^{10}&\triangleq\theta_{m,t}\mathbb{E}\{K_{m,t}\bar{y}_{m,t-1}\sqrt{\mathcal{R}_{m,t}}^T\lambda_{m,t}^T\bar{\varrho}_{m,t}^TK_{m,t}^T\},\\\mathcal{K}_{m,t}^{11}&\triangleq\theta_{m,t}^2\mathbb{E}\{K_{m,t}\bar{y}_{m,t-1}\tau_m^T(I-\bar{\varrho}_{m,t})^TK_{m,t}^T\},\\\mathcal{K}_{m,t}^{12}&\triangleq(1-\theta_{m,t})\mathbb{E}\{K_{m,t}\varepsilon_{m,t}\sqrt{\mathcal{R}_{m,t}}^T\lambda_{m,t}^T\bar{\varrho}_{m,t}^TK_{m,t}^T\},\\\mathcal{K}_{m,t}^{13}&\triangleq\theta_{m,t}\mathbb{E}\{K_{m,t}(I-\bar{\varrho}_{m,t})\tau_m\sqrt{\mathcal{R}_{m,t}}^T\lambda_{m,t}^T\bar{\varrho}_{m,t}^TK_{m,t}^T\}.\end{aligned}$$

Next, an upper bound for the filtering error covariance matrix $P_{m,t|t}$ is provided to eliminate the uncertainties in Eq. (27).

Theorem 1. *For the given positive scalars $\varepsilon_j\,(j=1,2,...,14)$, it is said that $\bar{P}_{m,t|t}$ is an upper bound of the $P_{m,t|t}$, namely,*

$$P_{m,t|t}\le\bar{P}_{m,t|t}, \tag{28}$$

with the initial value of $P_{0|0}=\bar{P}_{0|0}>0$. Moreover, $\bar{P}_{m,t|t}$ satisfies the following recursions:

$$\bar{P}_{m,t|t-1}=A_{t-1}\bar{P}_{m,t|t}A_{t-1}^T+B_{t-1}Q_{t-1}B_{t-1}^T, \tag{29}$$

and

$$
\begin{aligned}
\bar{P}_{m,t|t} =& \kappa_1(I - K_{m,t}\bar{\varrho}_{m,t}C_{m,t})\bar{P}_{m,t|t-1}(I - K_{m,t}\bar{\varrho}_{m,t}C_{m,t})^T + (1-\theta_{m,t})^2K_{m,t}\{\Omega_{m3,t}\circ R_{m,t}\}K_{m,t}^T \\
&+ \kappa_2K_{m,t}\bar{\varrho}_{m,t}\lambda_{m,t}\sqrt{\mathcal{R}_{m,t}}\sqrt{\mathcal{R}_{m,t}}^T\lambda_{m,t}^T\bar{\varrho}_{m,t}^TK_{m,t}^T + (1-\theta_{m,t})^2\kappa_3K_{m,t}C_{m,t}\{\Upsilon_{m,t}\circ\Omega_{m1,t}\}C_{m,t}^TK_{m,t}^T \\
&+ \theta_{m,t}^2\kappa_4K_{m,t}\bar{\varrho}_{m,t}C_{m,t}\Omega_{m1,t}C_{m,t}^T\bar{\varrho}_{m,t}^TK_{m,t}^T + \theta_{m,t}^2\kappa_5K_{m,t}\Omega_{m2,t}K_{m,t}^T \\
&+ (1-\theta_{m,t})^2\kappa_6K_{m,t}\Xi(\bar{G}_{m,t})K_{m,t}^T + \theta_{m,t}^2\kappa_7K_{m,t}(I-\bar{\varrho}_{m,t})\tau_m\tau_m^T(I-\bar{\varrho}_{m,t})^TK_{m,t+1}^T \\
&+ (1-\theta_{m,t})^2\kappa_8K_{m,t}\{\Upsilon_{m,t}\circ\tau_m\tau_m^T\}K_{m,t}^T
\end{aligned} \tag{30}
$$

where

$$
\begin{aligned}
\kappa_1 &\triangleq 1+\varepsilon_1+\varepsilon_2+\varepsilon_3+\varepsilon_4+\varepsilon_5, \\
\kappa_2 &\triangleq 1+\varepsilon_1^{-1}+\varepsilon_7^{-1}+\varepsilon_{10}^{-1}+\varepsilon_{12}^{-1}+\varepsilon_{13}^{-1}, \\
\kappa_3 &\triangleq 1+\varepsilon_6, \\
\kappa_4 &\triangleq 1+\varepsilon_7+\varepsilon_8+\varepsilon_9+\varepsilon_2^{-1}, \\
\kappa_5 &\triangleq 1+\varepsilon_3^{-1}+\varepsilon_8^{-1}+\varepsilon_{10}+\varepsilon_{11}, \\
\kappa_6 &\triangleq 1+\varepsilon_4^{-1}+\varepsilon_{12}, \\
\kappa_7 &\triangleq 1+\varepsilon_5^{-1}+\varepsilon_9^{-1}+\varepsilon_{11}^{-1}+\varepsilon_{13}, \\
\kappa_8 &\triangleq 1+\varepsilon_6^{-1}, \\
\Upsilon_{m,t} &\triangleq diag\{\bar{\varrho}_{m,t}^{(1)}(1-\bar{\varrho}_{m,t}^{(1)}),\cdots,\bar{\varrho}_{m,t}^{(n_y)}(1-\bar{\varrho}_{m,t}^{(n_y)})\}, \\
\Omega_{m1,t} &\triangleq (1+\varepsilon_{14})P_{t|t-1}+(1+\varepsilon_{14}^{-1})\hat{x}_{m,t|t-1}\hat{x}_{m,t|t-1}^T \\
\Omega_{m2,t-1} &\triangleq \bar{y}_{m,t-1}\bar{y}_{m,t-1}^T, \qquad \Omega_{m3,t} \triangleq \Upsilon_{m,t}+\bar{\varrho}_{m,t}\bar{\varrho}_{m,t}^T,
\end{aligned}
$$

and

$$
\begin{aligned}
\bar{G}_{m,t+1} &\triangleq \Xi(\bar{G}_{m,t}) \\
&= \left((1+d_t)(1+e_t)\lambda_m^2 + \frac{(1+\chi_m)(1+d_t^{-1})}{\chi_m^2}\right)\bar{G}_{m,t} + \left((1+d_t)(1+e_t^{-1})+(1+d_t^{-1})(1+\chi_m^{-1})\right)\sigma_m^2
\end{aligned}
$$

where $\bar{G}_{m,t}$ *is an upper bound of* $G_{m,t}\triangleq\mathbb{E}\{\eta_{m,t}^2\}$ *with the initial condition* $\bar{G}_{m,0}=\eta_{m,0}^2$.

Here, $\circ$ *denotes the Hadamard product, which is defined as* $[A\circ B]_{ij}=A_{ij}\cdot B_{ij}$.

Proof. According to lemma 1 in[36], it follows from Eq. (27) that

$$
\begin{aligned}
&P_{m,t|t} \\
\le&\kappa_1(I-K_{m,t}\bar{\varrho}_{m,t}C_{m,t})P_{m,t|t-1}(I-K_{m,t}\bar{\varrho}_{m,t}C_{m,t})^T + (1-\theta_{m,t})^2K_{m,t}\mathbb{E}\{\varrho_{m,t}v_{m,t}v_{m,t}^T\varrho_{m,t}^T\}K_{m,t}^T \\
&+ \kappa_2K_{m,t}\bar{\varrho}_{m,t}\mathbb{E}\{\lambda_{m,t}\sqrt{\mathcal{R}_{m,t}}\sqrt{\mathcal{R}_{m,t}}^T\lambda_{m,t}^T\}\bar{\varrho}_{m,t}^TK_{m,t}^T + (1-\theta_{m,t})^2\kappa_3K_{m,t}\mathbb{E}\{\tilde{\varrho}_{m,t}C_{m,t}x_tx_t^TC_{m,t}^T\tilde{\varrho}_{m,t}^T\}K_{m,t}^T \\
&+ \theta_{m,t}^2\kappa_4K_{m,t}\bar{\varrho}_{m,t}\mathbb{E}\{C_{m,t}x_tx_t^TC_{m,t}^T\}\bar{\varrho}_{m,t}^TK_{m,t}^T + \theta_{m,t}^2\kappa_5K_{m,t}\mathbb{E}\{\bar{y}_{m,t-1}\bar{y}_{m,t-1}^T\}K_{m,t}^T \\
&+ (1-\theta_{m,t})^2\kappa_6K_{m,t}\mathbb{E}\{\varepsilon_{m,t}\varepsilon_{m,t}^T\}K_{m,t}^T + \theta_{m,t}^2K_{m,t}\kappa_7(I-\bar{\varrho}_{m,t})\mathbb{E}\{\tau_m\tau_m^T\}(I-\bar{\varrho}_{m,t})^TK_{m,t+1}^T \\
&+ (1-\theta_{m,t})^2\kappa_8K_{m,t}\mathbb{E}\{\tilde{\varrho}_{m,t}\tau_m\tau_m^T\tilde{\varrho}_{m,t}^T\}K_{m,t}^T.
\end{aligned} \tag{31}
$$

Following the same line, one has

$$
\begin{aligned}
\mathbb{E}\{x_tx_t^T\} =&\mathbb{E}\{(e_{m,t|t-1}+\hat{x}_{m,t|t-1})(e_{m,t|t-1}+\hat{x}_{m,t|t-1})^T\} \\
\le&\mathbb{E}\{(1+\varepsilon_{14})e_{m,t|t-1}e_{m,t|t-1}^T+(1+\varepsilon_{14}^{-1})\hat{x}_{m,t|t-1}\hat{x}_{m,t|t-1}^T\} \\
\triangleq&\Omega_{m1,t}.
\end{aligned} \tag{32}
$$

Moreover, given the event-triggering condition (11), we have

$$\varepsilon_{m,t}^T\varepsilon_{m,t} \le \left(\frac{1}{\chi_m}\eta_{m,t} + \sigma_m\right)^2 \le (1+\chi_m)\chi_m^{-2}\eta_{m,t}^2 + (1+\chi_m^{-1})\sigma_m^2. \tag{33}$$

In light of lemma 5 and the proof of lemma 4 in[27], one derives

$$\mathbb{E}\{\varepsilon_{m,t}\varepsilon_{m,t}^T\} \le \Xi(\bar{G}_{m,t}). \tag{34}$$

Substituting Eqs. (32) and (34) into (31), one obtains the following inequality

$$\begin{aligned}
P_{m,t|t} \le& \kappa_1(I - K_{m,t}\bar{\varrho}_{m,t}C_{m,t})P_{m,t|t-1}(I - K_{m,t}\bar{\varrho}_{m,t}C_{m,t})^T + (1-\theta_{m,t})^2K_{m,t}\{\Omega_{m3,t}\circ R_{m,t}\}K_{m,t}^T \\
&+ \kappa_2K_{m,t}\bar{\varrho}_{m,t}\lambda_{m,t}\sqrt{\mathcal{R}_{m,t}}\sqrt{\mathcal{R}_{m,t}}^T\lambda_{m,t}^T\bar{\varrho}_{m,t}^TK_{m,t}^T + (1-\theta_{m,t})^2\kappa_3K_{m,t}C_{m,t}\{\Upsilon_{m,t}\circ\Omega_{m1,t}\}C_{m,t}^TK_{m,t}^T \\
&+ \theta_{m,t}^2\kappa_4K_{m,t}\bar{\varrho}_{m,t}C_{m,t}\Omega_{m1,t}C_{m,t}^T\bar{\varrho}_{m,t}^TK_{m,t}^T + \theta_{m,t}^2\kappa_5K_{m,t}\Omega_{m2,t}K_{m,t}^T \\
&+ (1-\theta_{m,t})^2\kappa_6K_{m,t}\Xi(\bar{G}_{m,t})K_{m,t}^T + \theta_{m,t}^2\kappa_7K_{m,t}(I-\bar{\varrho}_{m,t})\tau_m\tau_m^T(I-\bar{\varrho}_{m,t})^TK_{m,t+1}^T \\
&+ (1-\theta_{m,t})^2\kappa_8K_{m,t}\{\Upsilon_{m,t}\circ\tau_m\tau_m^T\}K_{m,t}^T.
\end{aligned} \tag{35}$$

By using lemma 2 in[27], one obtains that

$$P_{m,t|t} \le \bar{P}_{m,t|t}. \tag{36}$$

The proof is now complete. □

Next, the filter gain $K_{m,t}$ is designed such that $\mathrm{tr}\{\bar{P}_{m,t|t}\}$ is minimized at each time instant.

Theorem 2. *Suppose that the positive scalars $\varepsilon_j (j = 1, 2, ..., 14)$ are given. The upper bound of the filtering error covariance $\bar{P}_{m,t|t}$ given by Eq. (30) is minimized by the following filter gain*

$$K_{m,t} = \Psi_{m,t}\Phi_{m,t}^{-1} \tag{37}$$

where

$$\begin{aligned}
\Psi_{m,t} \triangleq& \kappa_1\bar{P}_{m,t|t-1}C_{m,t}^T\bar{\varrho}_{m,t}^T, \\
\Phi_{m,t} \triangleq& \kappa_1\bar{\varrho}_{m,t}C_{m,t}\bar{P}_{m,t|t-1}C_{m,t}^T\bar{\varrho}_{m,t}^T + \kappa_2\bar{\varrho}_{m,t}\lambda_{m,t}\sqrt{\mathcal{R}_{m,t}}\sqrt{\mathcal{R}_{m,t}}^T\lambda_{m,t}^T\bar{\varrho}_{m,t}^T \\
&+ \theta_{m,t}^2\left(\kappa_4\bar{\varrho}_{m,t}C_{m,t}\Omega_{m1,t}C_{m,t}^T\bar{\varrho}_{m,t}^T + \kappa_5\Omega_{m2,t} + \kappa_7(I-\bar{\varrho}_{m,t})\tau_m\tau_m^T(I-\bar{\varrho}_{m,t})^T\right) \\
&+ (1-\theta_{m,t})^2\left(\Omega_{m3,t}\circ R_{m,t} + \kappa_3C_{m,t}\{\Upsilon_{m,t}\circ\Omega_{m1,t}\}C_{m,t}^T + \kappa_8\{\Upsilon_{m,t}\circ(\tau_m\tau_m^T)\} + \kappa_6\Xi(\bar{G}_{m,t})\right).
\end{aligned}$$

Proof. First, calculate the trace of $\bar{P}_{m,t|t}$ obtained by Eq. (30) as follows

$$\begin{aligned}
&\mathrm{tr}(\bar{P}_{m,t|t}) \\
=&\mathrm{tr}\Big\{\kappa_1(I - K_{m,t}\bar{\varrho}_{m,t}C_{m,t})P_{m,t|t-1}(I - K_{m,t}\bar{\varrho}_{m,t}C_{m,t})^T + (1-\theta_{m,t})^2K_{m,t}\{\Omega_{m3,t}\circ R_{m,t}\}K_{m,t}^T \\
&+ \kappa_2K_{m,t}\bar{\varrho}_{m,t}\lambda_{m,t}\sqrt{\mathcal{R}_{m,t}}\sqrt{\mathcal{R}_{m,t}}^T\lambda_{m,t}^T\bar{\varrho}_{m,t}^TK_{m,t}^T + (1-\theta_{m,t})^2\kappa_3K_{m,t}C_{m,t}\{\Upsilon_{m,t}\circ\Omega_{m1,t}\}C_{m,t}^TK_{m,t}^T \\
&+ \theta_{m,t}^2\kappa_4K_{m,t}\bar{\varrho}_{m,t}C_{m,t}\Omega_{m1,t}C_{m,t}^T\bar{\varrho}_{m,t}^TK_{m,t}^T + \theta_{m,t}^2\kappa_5K_{m,t}\Omega_{m2,t}K_{m,t}^T \\
&+ (1-\theta_{m,t})^2\kappa_6K_{m,t}\Xi(\bar{G}_{m,t})K_{m,t}^T + \theta_{m,t}^2\kappa_7K_{m,t}(I-\bar{\varrho}_{m,t})\tau_m\tau_m^T(I-\bar{\varrho}_{m,t})^TK_{m,t+1}^T \\
&+ (1-\theta_{m,t})^2\kappa_8K_{m,t}\{\Upsilon_{m,t}\circ(\tau_m\tau_m^T)\}K_{m,t}^T\Big\}.
\end{aligned} \tag{38}$$

Next, one can derive the derivative of tr $\left\{\bar{P}_{m,t|t}\right\}$ as follows

$$\begin{aligned}
&\frac{\partial}{\partial K_{m,t}}\mathrm{tr}\left\{\bar{P}_{m,t|t}\right\}\\
=&-2\kappa_1(I-K_{m,t}\bar{\varrho}_{m,t}C_{m,t})\bar{P}_{m,t|t-1}C_{m,t}^T\bar{\varrho}_{m,t}^T+2(1-\theta_{m,t})^2K_{m,t}\{\Omega_{m3,t}\circ R_{m,t}\}\\
&+2\kappa_2K_{m,t}\bar{\varrho}_{m,t}\lambda_{m,t}\sqrt{\mathcal{R}_{m,t}}\sqrt{\mathcal{R}_{m,t}}^T\lambda_{m,t}^T\bar{\varrho}_{m,t}^T+2(1-\theta_{m,t})^2\kappa_3K_{m,t}C_{m,t}\{\Upsilon_{m,t}\circ\Omega_{m1,t}\}C_{m,t}^T\\
&+2\theta_{m,t}^2\kappa_4K_{m,t}\bar{\varrho}_{m,t}C_{m,t}\Omega_{m1,t}C_{m,t}^T\bar{\varrho}_{m,t}^T+2\theta_{m,t}^2\kappa_5K_{m,t}\Omega_{m2,t}\\
&+2(1-\theta_{m,t})^2\kappa_6K_{m,t}\Xi(\bar{G}_{m,t})+2\theta_{m,t}^2\kappa_7K_{m,t}(I-\bar{\varrho}_{m,t})\tau_m\tau_m^T(I-\bar{\varrho}_{m,t})^T\\
&+2(1-\theta_{m,t})^2\kappa_8K_{m,t}\{\Upsilon_{m,t}\circ(\tau_m\tau_m^T)\}.
\end{aligned}\tag{39}$$

By letting (39) be zero, one acquires the filter gain as follows:

$$\begin{aligned}
K_{m,t}=&\kappa_1\bar{P}_{m,t|t-1}C_{m,t}^T\bar{\varrho}_{m,t}^T\Big\{\kappa_1\bar{\varrho}_{m,t}C_{m,t}\bar{P}_{m,t|t-1}C_{m,t}^T\bar{\varrho}_{m,t}^T+(1-\theta_{m,t})^2\{\Omega_{m3,t}\circ R_{m,t}\}\\
&+\kappa_2\bar{\varrho}_{m,t}\lambda_{m,t}\sqrt{\mathcal{R}_{m,t}}\sqrt{\mathcal{R}_{m,t}}^T\lambda_{m,t}^T\bar{\varrho}_{m,t}^T+(1-\theta_{m,t})^2\kappa_3C_{m,t}\{\Upsilon_{m,t}\circ\Omega_{m1,t}\}C_{m,t}^T\\
&+\theta_{m,t}^2\kappa_4\bar{\varrho}_{m,t}C_{m,t}\Omega_{m1,t}C_{m,t}^T\bar{\varrho}_{m,t}^T+\theta_{m,t}^2\kappa_5\Omega_{m2,t}+(1-\theta_{m,t})^2\kappa_6\Xi(\bar{G}_{m,t})\\
&+\theta_{m,t}^2\kappa_7(I-\bar{\varrho}_{m,t})\tau_m\tau_m^T(I-\bar{\varrho}_{m,t})^T+(1-\theta_{m,t})^2\kappa_8\{\Upsilon_{m,t}\circ(\tau_m\tau_m^T)\}\Big\}^{-1}.
\end{aligned}\tag{40}$$

As such, one completes the proof of this theorem. □

Remark 3. *Different from the approach to dealing with the DETP in*[6,27,37]*, an indicator variable is employed to formulate the impact of the DETP. From (37), it can be observed that the filter gain $K_{m,t}$ is dependent on the indicator variable $\theta_{m,t}$, which formulates the combined role of DETP with the token bucket specifications. Meanwhile, the filter gain can be calculated under two cases, i.e., $\theta_{m,t}=1$ (i.e., filter does not receive measurement) and $\theta_{m,t}=0$ (i.e., filter does receive measurement), respectively.*

3.2. Boundedness analysis

In this section, the boundedness of $\bar{P}_{m,t|t}$ will be discussed in the sense of mean square. Before carrying out the performance analysis, an assumption is provided to make some necessary constraints on the corresponding parameters.

Assumption 1. *Suppose that the following inequalities hold*

$$\begin{aligned}
&\|A_t\|\le a,\quad \|B_t\|\le b,\quad \underline{c}\le\|C_{m,t}\|\le\bar{c},\quad \|\Upsilon_{m,t}\|\le\pi,\quad \|Q_{m,t}\|\le q,\quad \|\Xi(\bar{G}_{m,t+1})\|\le\rho,\\
&\|\tau_m\|\le\bar{\tau},\quad \|\Omega_{m1,t-1}\|\le\xi,\quad \|\Omega_{m2,t-1}\|\le\vartheta,\quad \|\Omega_{m3,t-1}\|\le o,\quad \underline{\varpi}\le\|\bar{\varrho}_{m,t}\|\le\bar{\varpi},\\
&\|R_{m,t}\|\le r,\quad \underline{\lambda}\le\|\lambda_{m,t}\|\le\bar{\lambda},\quad \left\|\sqrt{\mathcal{R}_{m,t}}\right\|\le\mu
\end{aligned}\tag{41}$$

where a, b, c, π, q, r, q, o, ρ, $\bar{\tau}$, ϑ, ξ, $\bar{c}$, $\underline{c}$, $\underline{\varpi}$, $\bar{\varpi}$, μ, and $\bar{\tau}$ are all known positive real numbers.

Theorem 3. *Suppose Assumption 1 holds, in line with the system (1) and censored measurement (2) under Assumption 1, if the following inequality holds:*

$$\kappa_1 w_{m,t}a^2<1,\tag{42}$$

where $w_{m,t}\triangleq\left\|I-K_{m,t}\bar{\varrho}_{m,t}C_{m,t}\right\|^2$, then the filtering error (25) is mean-square bounded. Moreover, one has

$$\lim_{t\to+\infty}\|\bar{P}_{m,t|t}\|=\frac{\Delta}{1-\kappa_1 w_{m,t}a^2}\tag{43}$$

where

$$\begin{aligned}\Delta \triangleq & \kappa_1 w_{m,t} b^2 q + (1-\theta_{m,t})^2 \bar{k}^2 ro + \kappa_2 \bar{k}^2 \overline{\varpi}^2 \bar{\lambda}^2 \mu^2 + (1-\theta_{m,t})^2 \kappa_3 \bar{k}^2 \bar{c}^2 \pi \xi \\ & + \theta_{m,t}^2 \kappa_4 \bar{k}^2 \overline{\varpi}^2 \bar{c}^2 \xi + \theta_{m,t}^2 \kappa_5 \bar{k}^2 \vartheta + (1-\theta_{m,t})^2 \kappa_6 \bar{k}^2 \rho \\ & + \theta_{m,t}^2 \kappa_7 \bar{k}^2 \bar{\tau}^2 + (1-\theta_{m,t})^2 \kappa_8 \bar{k}^2 \pi \bar{\tau}^2.\end{aligned}$$

Proof. In line with Assumption 1 and Eq. (26), it deduces that

$$\left\|\bar{P}_{m,t|t-1}\right\| \leq a^2 \left\|\bar{P}_{m,t-1|t-1}\right\| + b^2 q. \tag{44}$$

By noting Eqs. (37) with (40), the upper bound of the filter gain $K_{m,t+1}$ is given as

$$\left\|K_{m,t}\right\| \leq \left\|\Psi_{m,t}\right\| \left\|\Phi_{m,t}\right\|^{-1} \leq \frac{\overline{\varpi}\bar{c}}{\underline{\varpi}^2 \underline{c}^2} \triangleq \bar{k}, \tag{45}$$

from which can be gained from Eq. (30):

$$\begin{aligned}\left\|\bar{P}_{m,t|t}\right\| \leq & \kappa_1 \left\|I - K_{m,t} \bar{\varrho}_{m,t} C_{m,t}\right\|^2 \left\|\bar{P}_{m,t|t-1}\right\| + (1-\theta_{m,t})^2 \bar{k}^2 ro + \kappa_2 \bar{k}^2 \overline{\varpi}^2 \bar{\lambda}^2 \mu^2 \\ & + (1-\theta_{m,t})^2 \kappa_3 \bar{k}^2 \bar{c}^2 \pi \xi + \theta_{m,t}^2 \kappa_4 \bar{k}^2 \overline{\varpi}^2 \bar{c}^2 \xi + \theta_{m,t}^2 \kappa_5 \bar{k}^2 \vartheta + (1-\theta_{m,t})^2 \kappa_6 \bar{k}^2 \rho \\ & + \theta_{m,t}^2 \kappa_7 \bar{k}^2 \bar{\tau}^2 + (1-\theta_{m,t})^2 \kappa_8 \bar{k}^2 \pi \bar{\tau}^2.\end{aligned} \tag{46}$$

By means of $w_{m,t} \triangleq \left\|I - K_{m,t} \bar{\varrho}_{m,t} C_{m,t}\right\|^2$, one has

$$\begin{aligned}\left\|\bar{P}_{m,t|t}\right\| \leq & \kappa_1 w_{m,t} a^2 \left\|\bar{P}_{m,t-1|t-1}\right\| + \kappa_1 w_{m,t} b^2 q + (1-\theta_{m,t})^2 \bar{k}^2 ro + \kappa_2 \bar{k}^2 \overline{\varpi}^2 \bar{\lambda}^2 \mu^2 \\ & + (1-\theta_{m,t})^2 \kappa_3 \bar{k}^2 \bar{c}^2 \pi \xi + \theta_{m,t}^2 \kappa_4 \bar{k}^2 \overline{\varpi}^2 \bar{c}^2 \xi + \theta_{m,t}^2 \kappa_5 \bar{k}^2 \vartheta + (1-\theta_{m,t})^2 \kappa_6 \bar{k}^2 \rho \\ & + \theta_{m,t}^2 \kappa_7 \bar{k}^2 \bar{\tau}^2 + (1-\theta_{m,t})^2 \kappa_8 \bar{k}^2 \pi \bar{\tau}^2.\end{aligned} \tag{47}$$

In the following, we can rewrite (47) as follows

$$\|\bar{P}_{m,t|t}\| \leq \kappa_1 w_{m,t} a^2 \|\bar{P}_{m,t-1|t-1}\| + \Delta, \tag{48}$$

which further implies

$$\|\bar{P}_{m,t|t}\| \leq (\kappa_1 w_{m,t} a^2)^t \|\bar{P}_{m,0|0}\| + \frac{1-(\kappa_1 w_{m,t} a^2)^{t-1}}{1-\kappa_1 w_{m,t} a^2} \Delta. \tag{49}$$

If (42) holds, i.e., $\kappa_1 w_{m,t} a^2 < 1$, one then has (43), which implies that the convergence of the upper bound $\left\|\bar{P}_{m,t|t}\right\|$. Meanwhile, it is observed that $\bar{P}_{m,t|t}$ always serves as an upper bound for the true estimation error covariance $P_{m,t|t}$. Consequently, the filtering error is mean-square bounded. Therefore, the proof is now complete. □

Remark 4. *Theorem 3 shows the combined impact of the DETP with the token bucket specifications on the filtering error boundedness and the filtering accuracy. Noticing that $w_{m,t}$ is dependent on filter gain $K_{m,t}$ from sufficient condition (42) and $K_{m,t}$ is dependent on $\theta_{m,t}$ from (37), the DETP with the token bucket specifications will pose an impact on the bounded condition. In addition, as given in (43), $\theta_{m,t}$ and $w_{m,t}$ are involved in the upper bound of the filtering error covariance, showing that $\theta_{m,t}$ would also pose effect on the filtering accuracy.*

3.3. Federated Tobit Kalman fusion filtering

In line with federated filtering fusion, the state estimate and the error covariance are $\hat{x}_{m,t|t}$ and $\bar{P}_{m,t|t}$, respectively, produced by the mth LTKF. Let $\hat{x}^g_{t|t}$ and $\hat{P}^g_{t|t}$ denote the global optimal estimate and covariance obtained at the fusion center under the federated fusion rule.

Theorem 4. *The FTKFF scheme for systems (1)-(2) is expressed as*

$$\begin{cases} P^g_{t|t} = \left(\sum_{m=1}^{l} \bar{P}^{-1}_{m,t|t}\right)^{-1}, \\ \hat{x}^g_{t|t} = P^g_{t|t} \sum_{m=1}^{l} \bar{P}^{-1}_{m,t|t} \hat{x}_{m,t|t} \end{cases} \tag{50}$$

with the resulting updated values

$$\begin{cases} Q_{m,t} = \alpha_m^{-1} Q_t, \\ \bar{P}_{m,t|t} = \alpha_m^{-1} P^g_{t|t}, \\ \hat{x}_{m,t|t} = \hat{x}^g_{t|t} \end{cases} \tag{51}$$

where α_m is the information weight of the m-th local estimator and $\sum_{m=1}^{l} \alpha_m = 1$; $\hat{x}_{m,t|t}$, $\bar{P}_{m,t|t}$, and $Q_{m,t}$ are the local estimates, upper bounds, and process noise covariance to be initialized at time t for predictions at time $t+1$.

It is noted that the role of (51) is to allocate the fused result to the individual sub-filter. The detailed procedure of FTKFF is summarized in Algorithm 1.

In line with the boundedness analysis of Theorem 3, the same argument can be applied to deduce the boundedness.

According to Algorithm 1, one has the computational complexity of the scheme developed in this paper.

Remark 5. *Now, we focus on the computational complexity of the scheme. In light of the system dimensions, such as $x_t \in \mathbb{R}^{n_y}$, $y_{i,t} \in \mathbb{R}^{n_y}$, $w_t \in \mathbb{R}^{w}$ and the resulting matrix dimensions, such as $A_t \in \mathbb{R}^{n_x \times n_x}$, $B_t \in \mathbb{R}^{n_x \times n_w}$, $C_{i,t} \in \mathbb{R}^{n_y \times n_x}$, one can obtain the computational complexity of the scheme developed in this paper at every fixed time instant. The FLOPS (Floating Point Operations Per Second) of main computational formulas from Algorithm 1 is $7ln_y^3+(10l+1)n_x^3+36ln_y^2n_x+22ln_yn_x^2+(13l+6)n_x^2+18ln_y^2-17ln_xn_y-(2l+1)n_x-ln_y+2ln_xn_w^2-2ln_xn_w+2l+59$. The corresponding complexity is given as $O(7ln_y^3 + (10l+1)n_x^3 + 36ln_y^2n_x + 22ln_yn_x^2 + 2ln_xn_w^2)$.*

In the following, we will discuss the consistency of the federated fusion.

Theorem 5. *If $P_{m,t|t} \leq \bar{P}_{m,t|t}$, then one has*

$$\mathbb{E}\left\{(x_{t|t} - \hat{x}^g_{t|t})(x_{t|t} - \hat{x}^g_{t|t})^T\right\} \leq P^g_{t|t}. \tag{52}$$

Proof. First of all, one calculates

$$\begin{aligned} &\mathbb{E}\left\{(x_t - \hat{x}^g_{t|t})(x_t - \hat{x}^g_{t|t})^T\right\} \\ =&\mathbb{E}\left\{\left(x_t - P^g_{t|t}\sum_{m=1}^{l}\bar{P}^{-1}_{m,t|t}\hat{x}_{m,t|t}\right)\left(x_t - P^g_{t|t}\sum_{m=1}^{l}\bar{P}^{-1}_{m,t|t}\hat{x}_{m,t|t}\right)^T\right\} \\ =&P^g_{t|t}\mathbb{E}\left\{\left((P^g_{t|t})^{-1}x_t - \sum_{m=1}^{l}\bar{P}^{-1}_{m,t|t}\hat{x}_{m,t|t}\right)\left((P^g_{t|t})^{-1}x_t - \sum_{m=1}^{l}\bar{P}^{-1}_{m,t|t}\hat{x}_{m,t|t}\right)^T\right\}P^g_{t|t}. \end{aligned}$$

Algorithm 1 FTKFF

for m=1:l **do**
  Initialization: $\hat{x}_{m,0|0}$ and $\bar{P}_{m,0|0}$
end for
for t=1:N **do**
  for m=1:l **do**
    Execute information transmission protocols
    determine $\alpha_{m,t}$ by (15)
    determine $\beta_{m,t}$ by (18)
    if $\alpha_{m,t} = 1$ and $\beta_{m,t} = 1$ **then**
      $\bar{y}_{m,t} = y_{m,t_m^n}$
    else
      $\bar{y}_{m,t} = y_{m,t-1}$
    end if
    Execute Local filtering
    Calculate $\hat{x}_{m,t|t-1}$ by (21)
    Calculate $P_{m,t|t-1}$ by (29)
    Compute the filter gain $K_{m,t}$ in line with (37)
    Calculate $\hat{x}_{m,t|t}$ by (22)
    Compute $\bar{P}_{m,t|t}$ by (30)
  end for
  Execute fusion filtering
  Compute $P^g_{t|t}$ and $\hat{x}^g_{t|t}$ by (50)
  Update the number of tokens by (17)
  Tokens are assigned to every node by (16)
  Update $\hat{x}_{m,t|t}$ and $\bar{P}_{m,t|t}$ by (51)
end for

Noting such a fact:

$$\left(P^g_{t|t}\right)^{-1} = \sum_{m=1}^{l} \bar{P}^{-1}_{m,t|t},$$

one derives that

$$\begin{aligned}
&\mathbb{E}\left\{(x_t - \hat{x}^g_{t|t})(x_t - \hat{x}^g_{t|t})^T\right\} \\
=&P^g_{t|t}\mathbb{E}\left\{\left(\sum_{m=1}^{l}\bar{P}^{-1}_{m,t|t}x_t - \sum_{m=1}^{l}\bar{P}^{-1}_{m,t|t}\hat{x}_{m,t|t}\right)\left(\sum_{m=1}^{l}\bar{P}^{-1}_{m,t|t}x_t - \sum_{m=1}^{l}\bar{P}^{-1}_{m,t|t}\hat{x}_{m,t|t}\right)^T\right\}P^g_{t|t} \\
=&P^g_{t|t}\mathbb{E}\left\{\sum_{m=1}^{l}\bar{P}^{-1}_{m,t|t}\left(x_t - \hat{x}_{m,t|t}\right)\sum_{m=1}^{l}(x_t - \hat{x}_{m,t|t})^T\bar{P}^{-1}_{m,t|t}\right\}P^g_{t|t}.
\end{aligned}$$

According to (49), one further has

$$\bar{P}^{-1}_{m,t|t} = \alpha_m (P^g_{t|t})^{-1}, \tag{53}$$

which indicates that

$$
\begin{aligned}
&\mathbb{E}\left\{(x_t-\hat{x}^g_{t|t})(x_t-\hat{x}^g_{t|t})^T\right\}\\
=&P^g_{t|t}\mathbb{E}\left\{\sum_{m=1}^{l}\alpha_m(P^g_{t|t})^{-1}\left(x_t-\hat{x}_{m,t|t}\right)\sum_{m=1}^{l}(x_t-\hat{x}_{m,t|t})^T\alpha_m(P^g_{t|t})^{-1}\right\}P^g_{t|t}\\
=&\mathbb{E}\left\{\sum_{m=1}^{l}\alpha_m\left(x_t-\hat{x}_{m,t|t}\right)\sum_{m=1}^{l}\alpha_m(x_t-\hat{x}_{m,t|t})^T\right\}\\
=&\mathbb{E}\left\{\sum_{m=1}^{l}\sum_{s=1}^{l}\alpha_m\alpha_s\left(x_t-\hat{x}_{m,t|t}\right)\left(x_t-\hat{x}_{s,t|t}\right)^T\right\}.
\end{aligned}
\tag{54}
$$

By resorting to lemma 2 in[41], one derives

$$
\begin{aligned}
&\mathbb{E}\left\{(x_t-\hat{x}^g_{t|t})(x_t-\hat{x}^g_{t|t})^T\right\}\\
=&\mathbb{E}\left\{\sum_{m=1}^{l}\sum_{s=1}^{l}\alpha_m\alpha_s\left(x_t-\hat{x}_{m,t|t}\right)\left(x_t-\hat{x}_{s,t|t}\right)^T\right\}\\
\leq&\mathbb{E}\left\{\frac{1}{2}\sum_{m=1}^{l}\sum_{s=1}^{l}\alpha_m\alpha_s\left[\left(x_t-\hat{x}_{m,t|t}\right)\left(x_t-\hat{x}_{m,t|t}\right)^T+(x_t-\hat{x}_{s,t|t})(x_t-\hat{x}_{s,t|t})^T\right]\right\}\\
=&\sum_{m=1}^{l}\alpha_m\sum_{m=1}^{l}\alpha_m\mathbb{E}\left\{\left(x_t-\hat{x}_{m,t|t}\right)\left(x_t-\hat{x}_{m,t|t}\right)^T\right\}\\
=&\sum_{m=1}^{l}\alpha_m\sum_{m=1}^{l}\alpha_m P_{m,t|t}\\
\leq&\sum_{m=1}^{l}\alpha_m\sum_{m=1}^{l}\alpha_m\bar{P}_{m,t|t}\\
=&\sum_{m=1}^{l}\alpha_m P^g_{t|t}\\
=&P^g_{t|t}.
\end{aligned}
\tag{55}
$$

Now, the proof is complete. □

Remark 6. *The FTKFF scheme is proposed for a class of discrete time-varying systems under the schedule of the DETP with token bucket specifications. This paper embodies the following significant characteristics from two viewpoints: (1) a local Tobit Kalman filter (LTKFs) is elaborately designed based on an enhanced protocol model that gives combined consideration of the impacts incurred by the DETP and token bucket specifications, where two indicator variables are used to formulate their roles; (2) a federated fusion rule is chosen by productively integrating the local estimates from LTKFs.*

4. AN ILLUSTRATION EXAMPLE

In this section, an oscillator simulation example in[10,12] is provided to showcase the effectiveness of the proposed FTKFF algorithm, under the schedule of the dynamic event-triggering with tokens buckets. The system

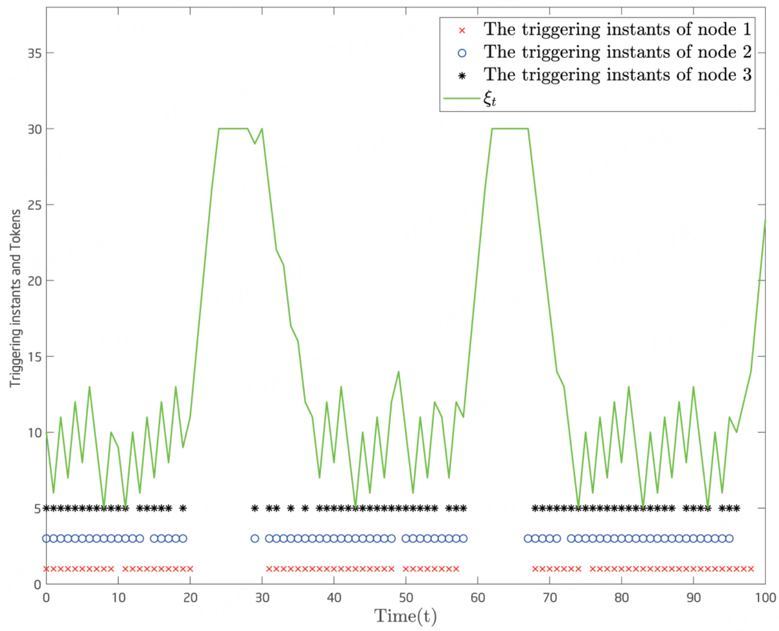

Figure 2. The dynamic change of token and triggering instants of three nodes.

parameters are chosen as

$$A_t = \begin{bmatrix} \cos(w) & \sin(w) \\ -\sin(w) & \cos(w) \end{bmatrix}, \quad B_t = \begin{bmatrix} 0.16 \\ 0.18 \end{bmatrix}, \quad w = 0.052\pi,$$

$$C_{1,t} = \begin{bmatrix} 1 & 0 \\ 0 & 1 \end{bmatrix}, C_{2,t} = \begin{bmatrix} 1 & 0 \\ 0 & 1 \end{bmatrix}, C_{3,t} = \begin{bmatrix} 1 & 0 \\ 0 & 1 \end{bmatrix}, x_0 = \begin{bmatrix} 5 \\ 0 \end{bmatrix},$$

$$Q_t = \mathrm{diag}\{0.05, 0.05\}, \quad R_{1,t} = R_{2,t} = R_{3,t} = 0.5.$$

In terms of the token bucket formulation, choose the following parameters

$$\beta_0 = 10, \quad c_1 = c_2 = c_3 = 3, \quad b = 30, \quad g = 5.$$

The corresponding parameters in the dynamic event-triggering conditions (14) are set to be $d_t = 1.5, e_t = 2$ $\sigma_1 = 0.1, \sigma_2 = 0.2, \sigma_3 = 0.3, \lambda_2 = 0.2, \lambda_1 = \lambda_3 = 0.1, \theta_1 = \theta_2 = \theta_3 = 5, \eta_{1,0} = \eta_{2,0} = \eta_{3,0} = 1.5,$ $a_1 = a_2 = a_3 = 1.5$, $b_1 = b_2 = b_3 = 2$. The threshold of τ_m is set to be a zero vector. In addition, set $\varepsilon_1 = \varepsilon_2 = \varepsilon_3 = \varepsilon_4 = \varepsilon_5 = 0.05, \varepsilon_i = 0.7 (i = 6, \cdots, 13)$, and $\varepsilon_{14} = 1$ for Eq. (32). By means of Theorems 2 and 3, one calculates the local filter gains $K_{i,t}$, the local estimates $\hat{x}_{m,t|t}$, and the global estimates $\hat{x}^g_{t|t}$, respectively.

The simulation results are displayed in Figures 2-10. Figure 2 depicts the utilization of communication resources under the schedule of dynamic event-triggered protocol with the token bucket specifications in the network, where the black asterisk, blue circle, and red cross are denoted as the event-triggering time instant of Node $i = 1, 2, 3$, and the green line represents the dynamic change of tokens. Figures 3 and 4 plot the censored measurements before and after the communication protocol scheduling, respectively, which reflects the role of scheduling in the information transmission. Figures 5-7 depict the local estimated values from every node and fusion estimation of state x_t. Figures 8-10 illustrate the logarithm (lg) of $e^T_{m,t|t} e_{m,t|t}$, $\mathrm{Tr}(\bar{P}_{m,t|t})$ for every sensor, $(e^g_{t|t})^T e^g_{t|t}$, and $\mathrm{Tr}(\bar{P}^g_{t|t})$.

In Figures 5-7, the blue curve represents the estimates from the local filters. Due to the existence of censored measurements, there exist obvious fluctuations of the local estimate, especially in the estimation of state $x^2_{3,t}$ in

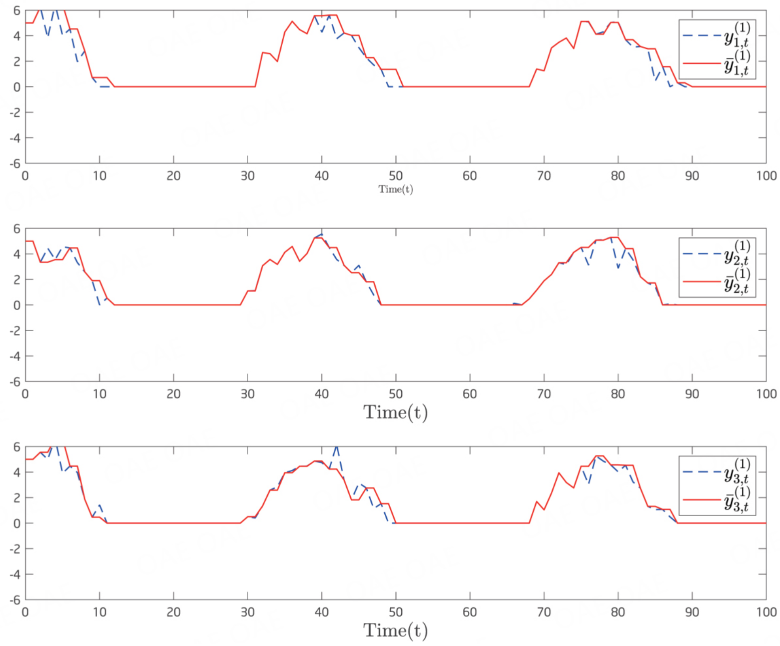

Figure 3. $y^1_{m,t}$ and $\bar{y}^1_{m,t}$.

Figure 7. However, federated fusion rules are used in this paper to obtain an optimal fusion estimate (shown by the red curve) by fully exploiting the estimates of all local filters. Meanwhile, the optimal fusion estimate can be fed back to the local filter to modify the fluctuations.

In Figures 8-10, the red curve represents the upper bound of the covariance of the local estimation error, while the yellow curve shows that of the filtering error after fusion. It can be observed that the result after fusion is better than that before fusion. Additionally, the blue dashed line represents the mean square error of the local estimator; the black curve indicates that after fusion. It can be noticed that in most cases, the mean square error of fused results is almost smaller than that of the local estimates, and the error curve is relatively smooth. This also demonstrates the superiority of the FTKFF scheme.

Thanks to the regulations of federated fusion filtering, distributed processing is achieved among sensors, where each local filter enhances the real-time performance of the system. Even in cases where a sensor fails or provides inaccurate information, the fusion center can enhance the filter's performance by utilizing data from other nodes and transmitting it to the local filter, resulting in a smoother filtered state value, which implies that the system becomes more resilient. As shown in Figures 8-10, the upper bound of the trace of the fused filtering error covariance matrix is smaller than that of a single node, and there is also an improvement in terms of mean square error. Therefore, the FTKFF scheme developed in this paper is indeed effective.

5. CONCLUSIONS

This paper has proposed a class of FTKFF schemes with censored measurements under the schedule of dynamic event-triggering with token specifications. First, the Tobit model has been used to describe the censored measurements. The token bucket traffic shaping algorithm with DETPs has been integrated to fully utilize limited communication resources. A local recursive filtering scheme has been designed for every node and an upper bound for the covariance matrix of the filtering error has been derived in the sense of trace. By minimizing this upper bound at each time step, the local filter gain has been calculated recursively. Additionally, sufficient conditions for the local filtering error to be mean-square stable are derived by analyzing the bounded-

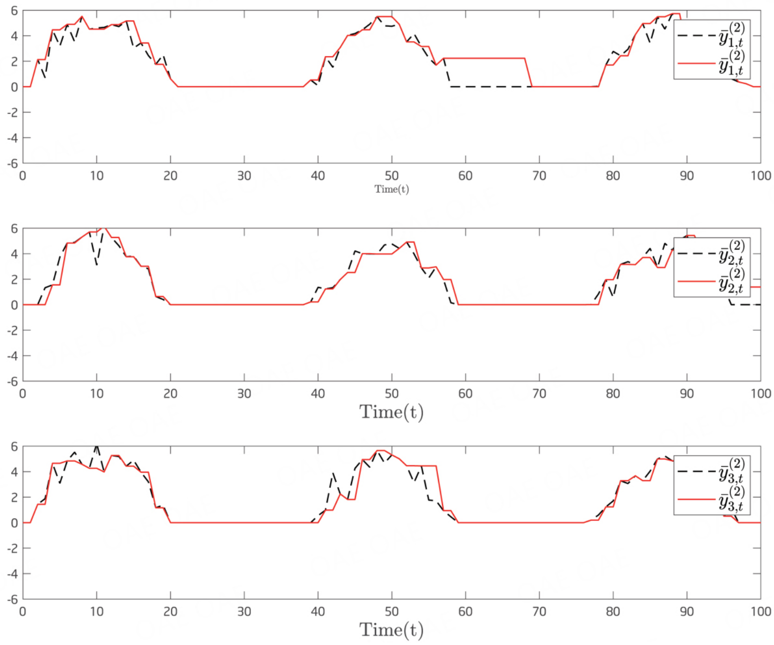

Figure 4. $y^2_{m,t}$ and $\bar{y}^2_{m,t}$.

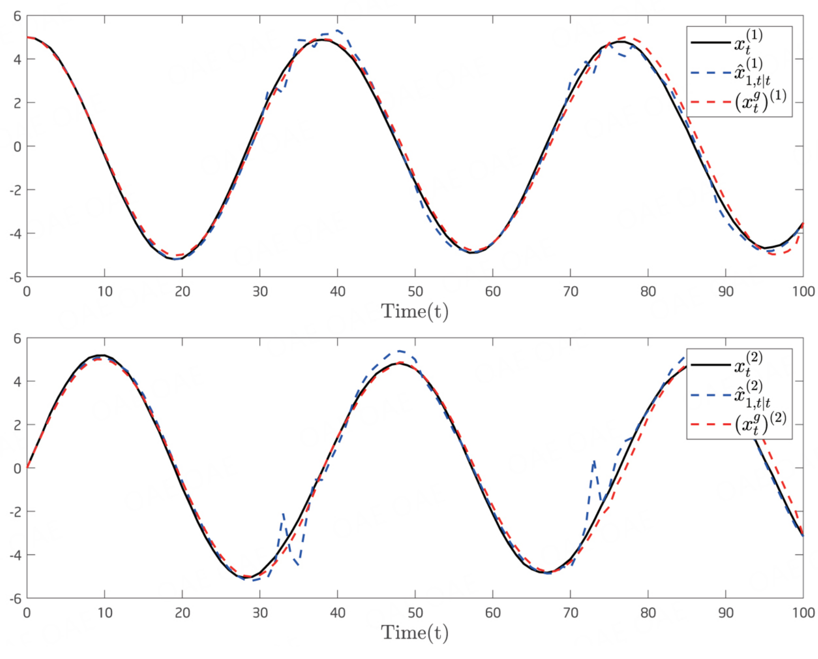

Figure 5. x_t, $\hat{x}_{1,t|t}$, and $\hat{x}^g_{t|t}$.

ness of the local filtering error covariance matrix. The fusion center processes the local filtering values at each time step via the federated fusion rule and distributes the fused results to each local filter. This comprehensive fusion filtering framework provides an effective solution to the censored measurements and information transmission protocol involving the DETP and token bucket specifications. Finally, the performance of the proposed FTKFF scheme is evaluated through a simulation example. In the future, the schemes proposed in this paper could be further developed to deal with more complicated cases such as sensor saturation, uncertain

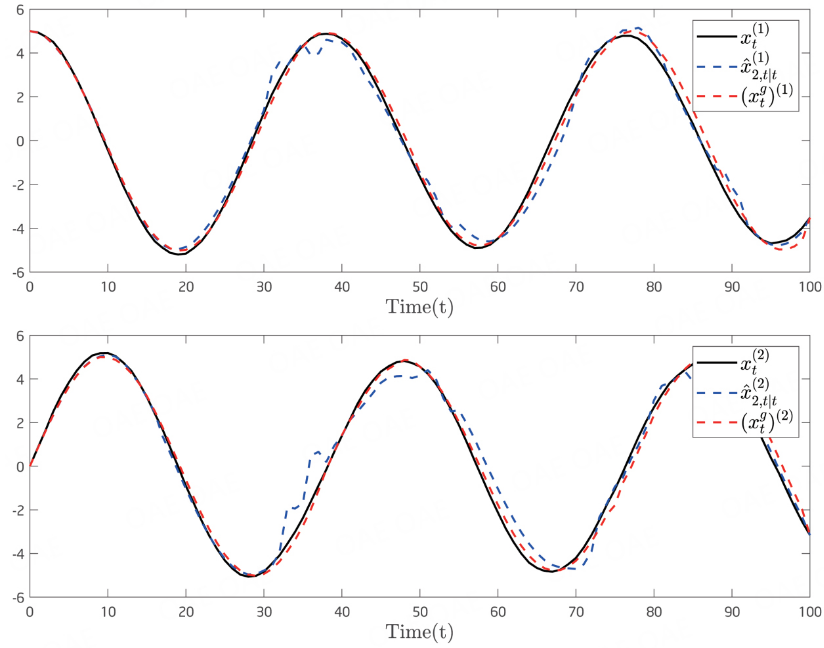

Figure 6. x_t, $\hat{x}_{2,t|t}$, and $\hat{x}^g_{t|t}$.

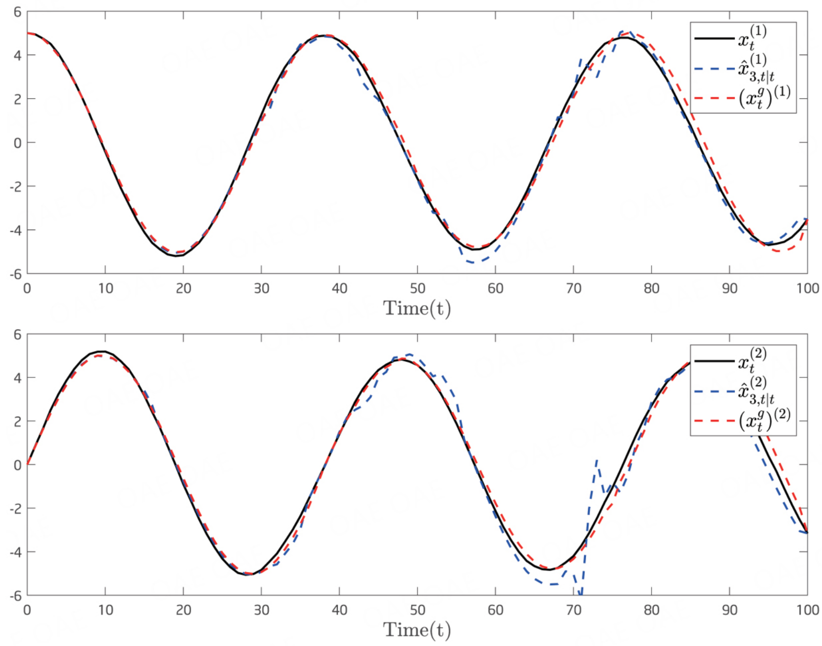

Figure 7. x_t, $\hat{x}_{3,t|t}$, and $\hat{x}^g_{t|t}$.

parameter systems, signal quantization, and time-delay systems or two-side censored measurements.

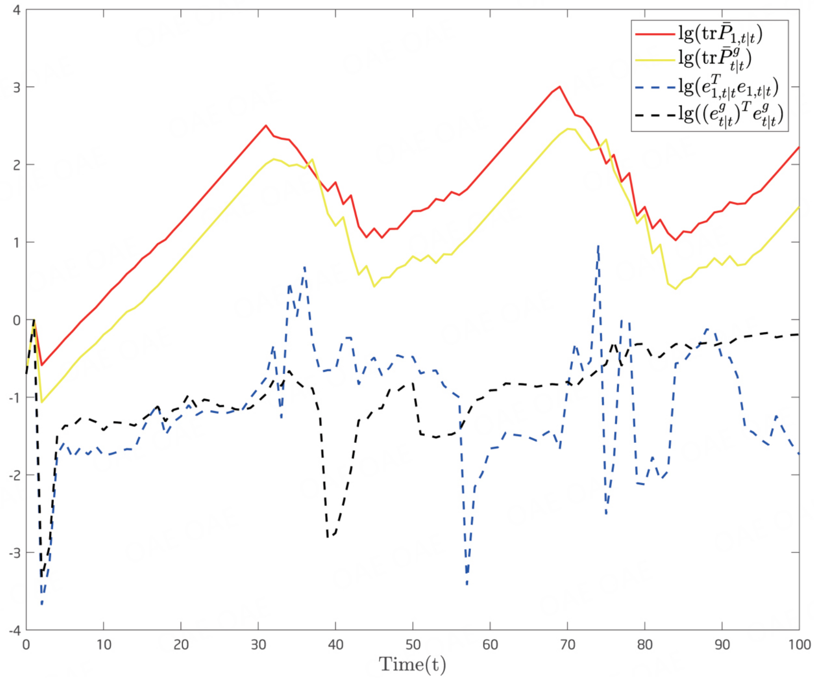

Figure 8. The logarithm of $e^{T}_{1,t|t}e_{1,t|t}$, $(e^{g}_{t|t})^{T}e^{g}_{t|t}$, tr$(\bar{P}_{1,t|t})$ and tr$(\bar{P}^{g}_{t|t})$.

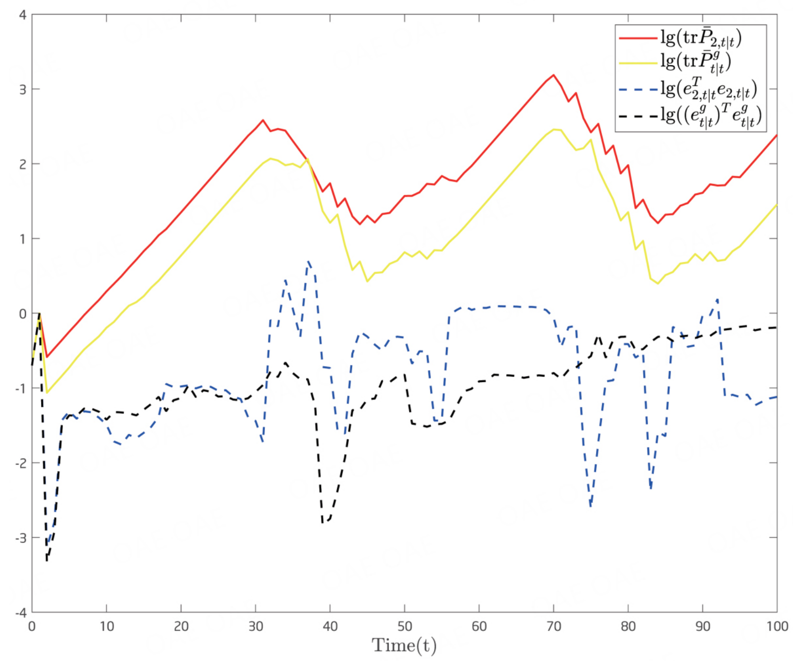

Figure 9. The logarithm of $e^{T}_{2,t|t}e_{2,t|t}$, $(e^{g}_{t|t})^{T}e^{g}_{t|t}$, tr$(\bar{P}_{2,t|t})$ and tr$(\bar{P}^{g}_{t|t})$.

DECLARATIONS

Authors' contributions

Conceptualization and manuscript drafting: Chen X
Methodology and experiment: Zhang J
Manuscript edition: Song Y
Review and supervision: Han F

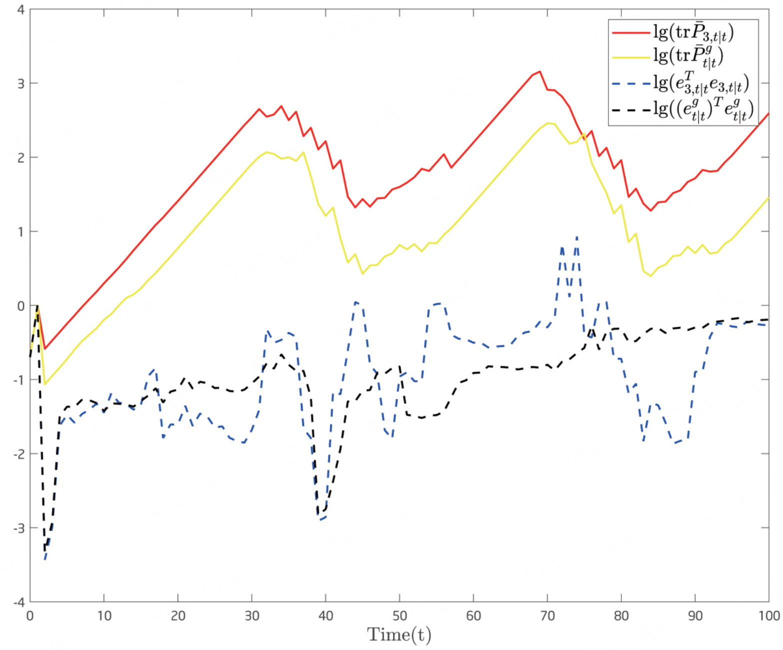

Figure 10. The logarithm of $e^T_{3,t|t}e_{3,t|t}$, $(e^g_{t|t})^T e^g_{t|t}$, tr$(\bar{P}_{3,t|t})$ and tr$(\bar{P}^g_{t|t})$.

Availability of data and materials
Not applicable.

Financial support and sponsorship
This work was supported in part by the National Natural Science Foundation of China under Grants 62073070 and U21A2019.

Conflicts of interest
Han F is a Junior Editorial Board Member of the journal *Complex Engineering Systems*, while the other authors have declared that they have no conflicts of interest.

Ethical approval and consent to participate
Not applicable.

Consent for publication
Not applicable.

REFERENCES

1. Li W, Yang F. Information fusion over network dynamics with unknown correlations: an overview. *Int J Netw Dyn Intell* 2023;2:100003. DOI
2. Jiang L, Yan L, Xia Y, Guo Q, Fu M, Lu K. Asynchronous multirate multisensor data fusion over inreliable measurements with correlated noise. *IEEE Trans Aerosp Electron Syst* 2017;53:2427-37. DOI
3. Li S, Deng Z, Feng X, He R, Pan F. Joint parameter and state estimation for stochastic uncertain system with multivariate skew t noises. *Chinese J Aeronaut* 2022;35:69-86. DOI
4. Darvishi H, Ciuonzo D, Eide ER, Rossi PS. Sensor-fault detection, isolation and accommodation for digital twins via modular data-driven architecture. *IEEE Sensors J* 2021;21:4827-38. DOI

5. Chen B, Ho DWC, Zhang WA, Yu L. Networked fusion estimation with bounded noises. *IEEE Trans Automat Control* 2017;62:5415-21. DOI
6. Niu Y, Sheng L, Gao M, Zhou D. Dynamic event-triggered state estimation for continuous-time polynomial nonlinear systems with external disturbances. *IEEE Trans Ind Inf* 2020;17:3962-70. DOI
7. Chen L, Bo K, Lee F, Chen Q. Advanced feature fusion algorithm based on multiple convolutional neural network for scene recognition. *Comput Model Eng Sci* 2020;122:505-23. DOI
8. Yan L, Li XR, Xia Y, Fu M. Optimal sequential and distributed fusion for state estimation in cross-correlated noise. *Automatica* 2013;49:3607-12. DOI
9. Shen Y, Wang Z, Shen B, Alsaadi FE. H_∞ filtering for multi-rate multi-sensor systems with randomly occurring sensor saturations under the p-persistent CSMA protocol. *IET Control Theory Appl* 2020;14:1255-65. DOI
10. Geng H, Wang Z, Alsaadi FE, Alharbi KH, Cheng Y. Federated Tobit Kalman filtering fusion with dead-zone-like censoring and dynamical bias under the round-robin protocol. *IEEE Trans Signal Inf Process Netw* 2020;7:1-16. DOI
11. Hu Z, Hu J, Tan H, Huang J, Cao Z. Distributed resilient fusion filtering for nonlinear systems with random sensor delay under round-robin protocol. *Int J Syst Sci* 2022;53:2786-99. DOI
12. Allik B, Miller C, Piovoso MJ, Zurakowski R. The Tobit Kalman filter: an estimator for censored measurements. *IEEE Trans Control Syst Technol* 2015;24:365-71. DOI
13. Hu J, Wang Z, Gao H. Recursive filtering with random parameter matrices, multiple fading measurements and correlated noises. *Automatica* 2013;49:3440-8. DOI
14. Shen Y, Wang Z, Shen B, Han QL. Recursive state estimation for networked multirate multisensor systems with distributed time-delays under round-robin protocol. *IEEE Trans Cyber* 2020;52:4136-46. DOI
15. Li X, Dong H, Wang Z, Han F. Set-membership filtering for state-saturated systems with mixed time-delays under weighted try-once-discard protocol. *IEEE Trans Circuits Syst II* 2018;66:312-6. DOI
16. Dai D, Li J, Song Y, Yang F. Event-based recursive filtering for nonlinear bias-corrupted systems with amplify-and-forward relays. *Syst Sci Control Eng* 2024;12:2332419. DOI
17. Jiang B, Gao H, Han F, Dong H. Recursive filtering for nonlinear systems subject to measurement outliers. *Sci China Inf Sci* 2021;64:172206. DOI
18. Wang Z, Liu Z, Dai Y, Cai K. Recursive estimation for system with random transmission loss and censored measurement. *IEEE Trans Circuits Syst II* 2022;70:2281-85. DOI
19. LoumponiaS K, Tsaklidis G. Kalman filtering with censored measurements. *J Appl Stat* 2022;49:317-35. DOI
20. Han F, Wang Z, Dong H. Partial-nodes-based scalable H_∞-consensus filtering with censored measurements. In: Distributed filtering, control and synchronization. studies in systems, decision and control. Cham: Springer; 2022. DOI
21. Li W, Jia Y, Du J. Tobit Kalman filter with time-correlated multiplicative measurement noise. *IET Control Theory Appl* 2017;11:122-8. DOI
22. Allik B, Miller C, Piovoso MJ, Zurakowski R. Nonlinear estimators for censored data: A comparison of the EKF, the UKF and the Tobit Kalman filter. In: 2015 American Control Conference (ACC). Chicago, USA, 2015; pp. 5146-51. DOI
23. Allik B, Miller C, Piovoso MJ, Zurakowski R. Estimation of saturated data using the Tobit Kalman filter. In: 2014 American control conference; Portland, OR, USA, 2014; pp. 4151-6. DOI
24. Han F, Dong H, Wang Z, Li G, Alsaadi FE. Improved Tobit Kalman filtering for systems with random parameters via conditional expectation. *Signal Process* 2018;147:35-45. DOI
25. Zou L, Wang Z, Han QL, Zhou D. Moving horizon estimation for networked time-delay systems under round-robin protocol. *IEEE Trans Automat Control* 2019;64:5191-98. DOI
26. Wen C, Wang Z, Liu Q, Alsaadi FE. Recursive distributed filtering for a class of state-saturated systems with fading measurements and quantization effects. *IEEE Trans Syst Man Cyber Syst* 2018;48:930-41. DOI
27. Li Q, Wang Z, Li N, Sheng W. A dynamic event-triggered approach to recursive filtering for complex networks with switching topologies subject to random sensor failures. *IEEE Trans Neural Netw Learn Syst* 2020;31:4381-8. DOI
28. Li XR, Zhu Y, Wang J, Han C. Optimal linear estimation fusion .I. Unified fusion rules. *IEEE Trans Inf Theory* 2003;49:2192-208. DOI
29. Song E, Zhu Y, Zhou J, You Z. Optimal Kalman filtering fusion with cross-correlated sensor noises. *Automatica* 2007; 43:1450-6. DOI
30. Zhang Y, Chen B, Yu L. Fusion estimation under binary sensors. *Automatica* 2020;115:108861. DOI
31. Shen Y, Wang Z, Shen B, Alsaadi FE, Alsaadi FE. Fusion estimation for multi-rate linear repetitive processes under weighted try-once-discard protocol. *Inf Fusion* 2020;55:281-91. DOI
32. Lin H, Sun S. Optimal sequential fusion estimation with stochastic parameter perturbations, fading measurements, and correlated noises. *IEEE Trans Signal Process* 2018;66:3571-83. DOI
33. Shen B, Wang Z, Tan H, Chen H. Robust fusion filtering over multisensor systems with energy harvesting constraints. *Automatica* 2021;131:109782. DOI
34. Geng H, Liu H, Ma L, Yi X. Multi-sensor filtering fusion meets censored measurements under a constrained network environment: advances, challenges and prospects. *Int J Syst Sci* 2021;52:3410-36. DOI
35. Sun J, Shen B, Liu Y. A resilient outlier-resistant recursive filtering approach to time-delayed spatial–temporal systems with energy harvesting sensors. *ISA Trans* 2022;127:41-9. DOI
36. Hu G, Wang Z, Alsaadi FE, Hayat T. Event-based filtering for time-varying nonlinear systems subject to multiple missing measurements with uncertain missing probabilities. *Inf Fusion* 2017;38:74-83. DOI

37. Han F, Wang Z, Dong H, Alsaadi FE, Alharbi KH. A local approach to distributed H_∞-consensus state estimation over sensor networks under hybrid attacks: Dynamic event-triggered scheme. *IEEE Trans Signal Inf Process Netw* 2022;8:556-70. DOI
38. Wildhagen S, Müller MA, Allgöwer F. Predictive control over a dynamical token bucket network. *IEEE Control Syst Lett* 2019;3:859-64. DOI
39. Khashooei AB, Antunes DJ, Heemels WPMH. Output-based event-triggered control with performance guarantees. *IEEE Trans Automat Control* 2017;62:3646-52. DOI
40. Linsenmayer S, Carabelli BW, Wildhagen S, Rothermel K, Allgöwer F. Controller and triggering mechanism co-design for control over time-slotted networks. *IEEE Trans Control Netw Syst* 2021;8:222-32. DOI
41. Liu Y, Wang Z, Liang J, Liu X. Synchronization and state estimation for discrete-time complex networks with distributed delays. *IEEE Trans Syst Man Cyber Part B* 2008;38:1314-25. DOI